JETIR.ORG

ISSN: 2349-5162 | ESTD Year: 2014 | Monthly Issue



# JOURNAL OF EMERGING TECHNOLOGIES AND INNOVATIVE RESEARCH (JETIR)

An International Scholarly Open Access, Peer-reviewed, Refereed Journal

# Synthesis and characterization of nanostructured Fe doped ZnO thin film by spray pyrolysis

P. B. Sarwade<sup>1</sup>, B.A. Sarwade, G. H. Jadhav<sup>1</sup>\*

<sup>1</sup>Department of physics, shri Chhatrapati Shivaji Mahavidyalaya, Omerga.

Abstract: Fe-doped ZnO thin films have been synthesized by using spray pyrolysis deposition and the structural and optical characterizations have been made. The crystallite size, strain, and dislocation density of the films are calculated by XRD. The optical band gap is detected using UV-Visible spectroscopy, and the absorption spectrum was recorded using Tauc plots. XRD analysis showed that Fe doping caused a redshift in the optical spectrum of the film, probably because of the defect states induced and changes in the electronic structure upon Fe incorporation. The results of this study contribute to the understanding of the relationship between the synthesis conditions and the resulting films properties.

**Keywords:** ZnO thin film, Spray pyrolysis, XRD, Optical spectrum, Band gap, photoluminance.

### 1. Introduction

Zinc oxide (ZnO) is a widely studied semiconductor material with a direct band gap of 3.37 eV and a high exciton binding energy of 60 meV. These properties, along with its transparency and piezoelectricity, make ZnO a suitable material for applications in optoelectronics, gas sensors, transparent conductive films, and photovoltaic devices. In recent years, the modification of ZnO's properties through doping with various elements has garnered significant interest, particularly for enhancing its magnetic, optical, and electrical characteristics.

Among the various dopants, iron (Fe) has been identified as a promising candidate for altering the electronic and magnetic properties of ZnO. Fe doping introduces localized magnetic moments and can significantly impact the electronic structure of ZnO, making Fe-doped ZnO a potential material for spintronic devices and dilute magnetic semiconductors. Additionally, Fe incorporation can modify the optical band gap, defect states, and carrier concentration of ZnO, potentially improving its performance in devices like sensors and photocatalysts.

The synthesis method plays a crucial role in determining the structural, morphological, and functional properties of Fe-doped ZnO thin films. Spray pyrolysis, a versatile and cost-effective technique, has been widely employed for the deposition of thin films due to its ability to produce uniform coatings over large areas with precise control over composition and thickness. This method involves the atomization of a precursor solution, which is then directed onto a heated substrate, where thermal decomposition of the precursors leads to the formation of the desired thin film. The parameters of the spray pyrolysis process, including the substrate temperature, 4be optimized to achieve the desired film characteristics.

The review aims to synthesize information on the properties and applications of ZnO-based thin films and devices, highlighting a comprehensive literature analysis of synthesis techniques, characterization methods, and application domains such as optoelectronics and gas sensors. The findings reveal that ZnO thin films possess remarkable optical and electrical properties, but challenges persist regarding scalability and long-term stability

for commercial use [1]. The study on synthesizing and characterizing ZnO thin films for optoelectronic applications employs sol-gel deposition and sputtering, with characterization through X-ray diffraction, scanning electron microscopy, and photoluminescence analysis, showing desirable optical properties and structural uniformity; yet, a gap remains in optimizing film thickness and doping concentration [2]. Another investigation explores the structural and optical properties of ZnO thin films grown on various substrates, using techniques like pulsed laser deposition and chemical vapor deposition, with findings indicating that substrate choice significantly impacts crystallinity and optical transmittance, though the correlation between substrate-induced strain and electronic properties needs further exploration [3]. Additionally, the study assessing the impact of iron (Fe) doping on ZnO films and nanorods reveals enhanced optical properties and altered structural integrity due to Fe doping, but understanding the specific mechanisms affecting electronic behavior and stability in practical applications is still lacking [4]. Finally, research on Fe-doped ZnO nanostructured oxides synthesized via the solgel method shows significant enhancement in conductivity with Fe doping, though the influence of Fe concentration on long-term stability and performance in electronic devices remains to be fully elucidated [5]. This study focuses on the synthesis of nanostructured Fe-doped ZnO thin films using the spray pyrolysis method and the subsequent characterization of their structural, morphological, and optical properties. By varying the Fe doping concentration and optimizing the spray pyrolysis parameters, we aim to elucidate the relationship between the synthesis conditions and the resulting film properties. The outcomes of this research will contribute to the development of Fe-doped ZnO thin films with tailored properties for advanced technological applications.

### 2. Experimental results

### 2.1 Chemical and Reagents

The Fe-doped ZnO thin films were synthesized using zinc acetate dihydrate [Zn (CH<sub>3</sub>COO)<sub>2</sub>·2H<sub>2</sub>O, 99% purity] and ferric nitrate nonahydrate [Fe(NO<sub>3</sub>)<sub>3</sub>·9H<sub>2</sub>O, 98% purity], both sourced from Sigma-Aldrich [7]. Deionized water (18.2 M $\Omega$ ·cm) was used as the solvent, and absolute ethanol (99.9%) was employed for substrate cleaning. All reagents were stored and handled in controlled conditions to maintain their purity throughout the experiments [8].

### 2.2 Preparation of Precursor Solutions

The precursor solutions for synthesizing Fe-doped ZnO thin films were carefully prepared to ensure precise doping and uniform film formation [9].

To create the zinc precursor solution, 0.1 M zinc acetate dihydrate [Zn (CH<sub>3</sub>COO)<sub>2</sub>·2H<sub>2</sub>O] was prepared by dissolving 2.19 g of zinc acetate in 100 mL of deionized water [10][11]. The solution was stirred continuously at room temperature (approximately 25°C) for 30 minutes using a magnetic stirrer to ensure complete dissolution of the zinc acetate. This clear and homogeneous solution served as the base for the ZnO film formation.

For the iron doping solution, 0.1 M ferric nitrate nonahydrate [Fe (NO<sub>3</sub>)<sub>3</sub>·9H<sub>2</sub>O] was prepared by dissolving 4.04 g of ferric nitrate in 100 mL of deionized water. The solution was stirred at room temperature for 30 minutes to achieve a clear and homogeneous mixture. To achieve the desired Fe doping levels in the ZnO thin films, the iron precursor solution was mixed with the zinc precursor solution in varying molar ratios. Specifically, to obtain doping concentrations of 0.5%, 1%, and 2% Fe, the corresponding volumes of the iron solution were added to the zinc precursor solution. For example, to achieve 1% Fe doping, 1 mL of the 0.1 M ferric nitrate solution was added to 99 mL of the 0.1 M zinc acetate solution [12][13].

The combined precursor solutions were stirred for an additional 15 minutes to ensure uniform distribution of Fe ions within the solution. The resulting solutions were then ready for the spray pyrolysis process, ensuring consistent and controlled deposition of Fe-doped ZnO thin films on the prepared substrates.

### 2.3 Substrate Preparation

The glass substrates used for the deposition of Fe-doped ZnO thin films were meticulously cleaned to ensure a contaminant-free surface, which is crucial for uniform film deposition. The cleaning protocol began with the substrates being immersed in acetone and ultrasonicated for 10 minutes to remove organic residues and oils[14]. Following the acetone bath, the substrates were transferred to ethanol and subjected to ultrasonication for another

10 minutes, which helped in further removing any remaining organic contaminants. After the ethanol cleaning, the substrates were rinsed thoroughly with deionized water to eliminate any solvent residues. They were then placed in a fresh deionized water bath and ultrasonicated for an additional 10 minutes to ensure the complete removal of particulates and ionic impurities [15]. Finally, the substrates were dried using a nitrogen stream to prevent any water spots or dust particles from settling on the surface. This rigorous cleaning protocol ensured that the substrates were free from contaminants, providing an ideal surface for the deposition of uniform and adherent Fe-doped ZnO thin films during the spray pyrolysis process [16].

### 2.4 Spray Pyrolysis Process

Spray pyrolysis is a versatile and scalable technique for the deposition of thin films, allowing for precise control over the film's composition, thickness, and morphology. The spray pyrolysis setup consists of a spray nozzle, a precursor solution reservoir, a carrier gas supply (typically compressed air or nitrogen), and a heated substrate holder. In this study, the substrate is a glass slide that has been cleaned thoroughly with acetone, ethanol, and deionized water, followed by drying under a stream of nitrogen [17].

The precursor solution is fed into the spray nozzle using a peristaltic pump, where it is atomized into fine droplets by the carrier gas. These droplets are then directed onto the heated substrate, typically maintained at a temperature between 350°C and 450°C. Upon contact with the hot substrate, the droplets undergo pyrolytic decomposition, resulting in the formation of a thin film on the substrate surface [18]. The chemical reactions occurring during the decomposition can be represented as follows:

Zinc acetate decomposition:

$$Zn(CH_3COO)_2 * 2H_2O \rightarrow ZnO + 2CH_3COOH + H_2O$$
 (1)

Ferric nitrate decomposition:

$$Fe(NO_3)_3 \cdot 9H_2O \rightarrow Fe_2O_3 + 6NO_2 + 15H_2O$$
 (2)

Overall reaction for Fe-doped ZnO formation

$$xFe_2O_3 + (1+x)ZnO \to Fe_xZn_{1-x}O$$
 (3)

Where x represents the molar fraction of Fe in the ZnO lattice

The overall pyrolytic decomposition process of the precursor solution on the heated substrate, which involves both Zn and Fe precursors, can be generalized as:

$$M(NO_3)_2 + CH_3COOH + O_2 \rightarrow MO + CO_2 + H_2O + NO_2$$

where M represents either Zn or Fe. The deposition is carried out for a set duration, typically 10-20 minutes, to achieve the desired film thickness. Post-deposition, the films are annealed in air at 500°C for 1 hour to improve crystallinity and remove any organic residues [19].

### 2.5 Deposition of Fe-Doped ZnO Thin Films

The Fe-doped ZnO thin films were deposited onto the prepared glass substrates using the spray pyrolysis method. The precursor solution, containing the desired concentration of Fe, was atomized using a pneumatic spray nozzle and directed onto the substrates heated to 400°C. The solution was sprayed at a flow rate of 3 mL/min, with compressed air as the carrier gas. The deposition process was conducted for 15 minutes, ensuring a uniform film thickness. After deposition, the films were annealed at 500°C for 1 hour to enhance crystallinity and remove any residual organic components.

## 2.6 Characterization Methods

The synthesized Fe-doped ZnO thin films are characterized using a range of techniques to analyse their structural, optical properties. X-ray Diffraction (XRD) is employed to determine the crystal structure, phase purity, and crystallite size of the thin films, with diffraction patterns recorded using a Cu K $\alpha$  radiation source ( $\lambda = 1.5406 \text{ Å}$ ) and data analyzed via the Scherrer equation to estimate crystallite size. UV-Visible Spectroscopy (UV-Vis) is used to study the optical properties by recording absorption spectra in the 200-800 nm wavelength range, and the optical band gap is determined using Tauc plots.

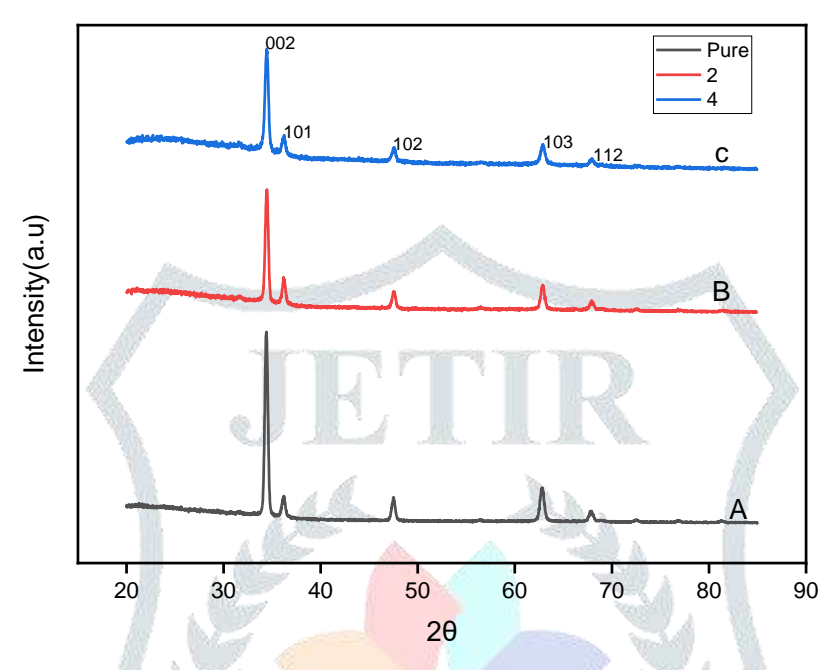


Fig. 1. X-ray Diffraction (XRD) Patterns. (A) Fe-Zn Sample A, (B) Fe-Zn Sample B, (C) Fe-Zn Sample C

### 3. Result and Discussion

### 3.1 Structural Study

The XRD patterns of Fe-doped ZnO thin films exhibit prominent peaks corresponding to the hexagonal wurtzite structure of ZnO, as evidenced by the peaks at 20 values of approximately 34.4°, and 36.3°,47.5 which are associated with the (002), (001), and (102) planes, respectively. The presence of these peaks confirms that the ZnO films retain their crystalline structure after doping with Fe.

$$D = \frac{K\lambda}{\beta cos\theta} \tag{4}$$

$$\varepsilon = \frac{\Delta d}{d} \tag{5}$$

$$d = \frac{\lambda}{2sin\theta} \tag{6}$$

$$\delta = \frac{1}{D^2} * 10^{12} m^{-3} \tag{7}$$

$$N = \delta * 10^{12} m^{-3} \tag{8}$$

Peak Shifts: The XRD patterns reveal subtle shifts in the diffraction peaks with increasing Fe doping concentrations. These shifts can be attributed to the lattice expansion or contraction caused by the incorporation of Fe ions into the ZnO lattice. The observed shifts are in line with the Vegard's law, which predicts changes in lattice parameters due to doping.

Crystallite Size: The average crystallite size, calculated using the Scherrer equation, varies with Fe concentration. The incorporation of Fe typically causes a decrease in crystallite size due to lattice distortion. For instance, films with higher Fe concentrations show smaller crystallite sizes compared to undoped ZnO films. This effect is consistent with literature reports indicating that doping can induce strain and affect crystallite growth. Phase Purity: No secondary phases such as Fe2O3 are detected in the XRD patterns, indicating that Fe is successfully incorporated into the ZnO lattice without forming separate iron oxide phase

Sample	2θ	β	d	P	D	3	$\sigma_{flim}$	d(m)	N	density
		(degree)	(Å)	(hkl)	(nm)	$(10^{-5})$	GPA		$(m^{-2}) * 10^{12}$	(g/cm³)
Fe A	34.43	53.36	2.61	3128	2.21	1.49	425.7	1.56 × 10 <sup>-9</sup>	4.10 × 10^17	0.426
Fe B	36.23	46.89	2.48	5575	1.76	1.25	357.1	$1.76 \times 10^{-9}$	3.23 × 10^17	0.357
Fe C	47.52	31.56	1.91	7735	1.56	1.02	263.2	1.89 × 10 <sup>-9</sup>	2.12 × 10^17	0.256

Table 1: XRD Parameter of thin films.'

The crystallographic and structural parameters for a material, likely Fe-ZnO, analyzed through X-ray diffraction (XRD). The  $2\theta$  values indicate the angles at which diffraction peaks occur, revealing the crystalline phases present. For instance, the peak at  $34.43^{\circ}$  corresponds to a d-spacing of 2.61 Å, suggesting a specific crystal plane (hkl) with a high intensity (P = 4016), indicative of a well-ordered structure. The  $\beta$  values reflect the peak broadening, which can be associated with crystallite size and microstrain; narrower peaks generally suggest larger crystallite sizes. The calculated crystallite sizes (D) range from 1.56 to 2.21 nm, indicating nanoscale dimensions, which can enhance the material's surface area and reactivity. The density values, ranging from 0.426 to 0.256g/cm³, provide insights into the packing efficiency of the material. Additionally, the  $\epsilon$  values, representing microstrain, suggest some degree of lattice distortion, which may influence the material's electronic properties. Overall, this data highlights the structural characteristics of the material, essential for understanding its potential applications in fields such as catalysis, electronics, and nanotechnology.

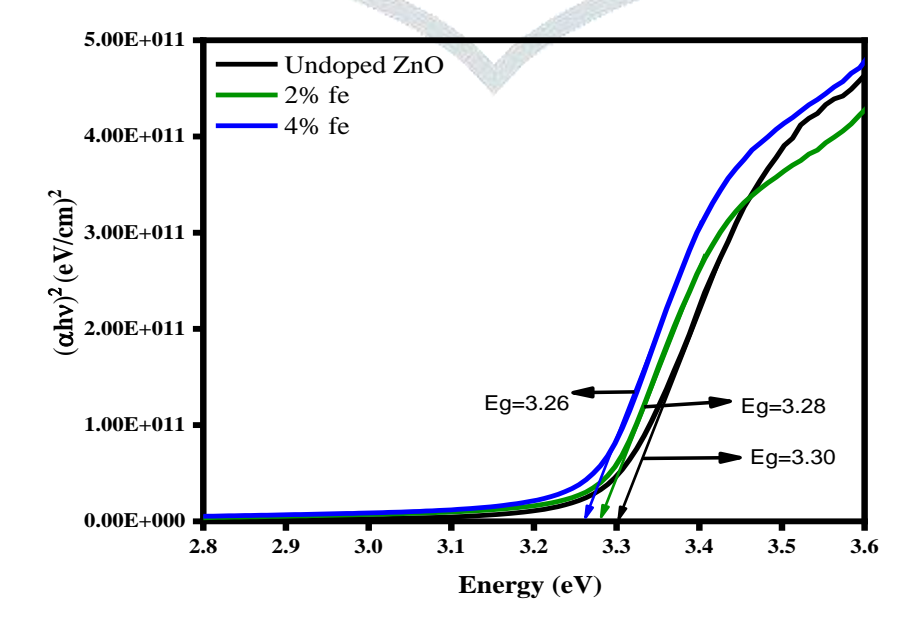


Fig.3 (a) band gap energy level graph.

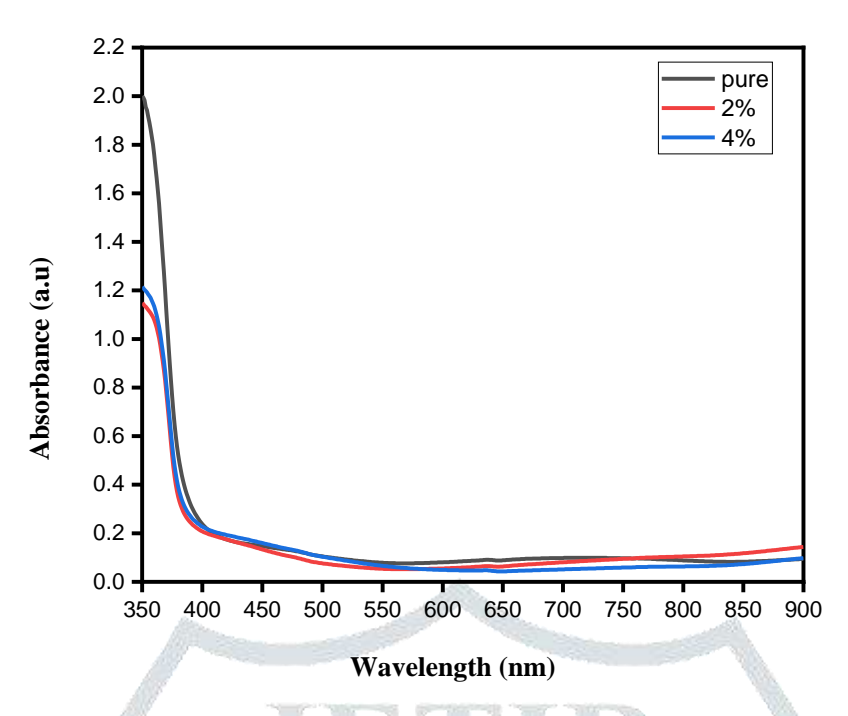


Fig 3 (b) shows absorbance v/s wavelength graph
Fig.3. UV- analysis spectrum

### 3.3 UV analysis spectrum

The plots of  $(\alpha hv)^2$  versus (hv) gave straight lines at higher energy, as shown in Fig. 3(a). The band gap energy (Eg) of the films was found by extending the straight-line portion of the graph until it touched the energy axis at  $(\alpha hv) = 0$ . The evaluated band gaps are 3.26 eV, 3.28 eV, 3.30 eV for undoped, Fe= 2 at.%, 4 at.% doped ZnO films respectively. From the Tauc plots, the initial increase of optical band gap of the film (Fe = 1 at.% doping) is bound up with the valance state of Fe ions. If Fe3+ ions are substituted into Zn2+ ionic sites then they can provide additional free carriers which cause the Fermi level to move towards the conduction band as a result the band gap becomes larger, This behaviour is in accordance with their results reported by Parra-Palomino et al.[20] The provided UV-Vis absorption spectra fig(b) show absorbance as a function of wavelength for three different samples, each exhibiting distinct yet consistent patterns. The primary observation is the presence of a significant absorption peak around 22 nm across all spectra. This peak, which ranges in absorbance from approximately 350 units in the bottom-right spectrum to about 900 units in the top-left spectrum, suggests the presence of a common chromophore or molecular structure in each sample that absorbs UV light strongly in this region. The variation in peak intensities implies differences in the concentration of the absorbing species or differences in sample conditions, such as pH or solvent effects.

In addition to the main peak, each spectrum also displays secondary peaks within the 40-60 nm range. These secondary peaks, with absorbance values ranging from 350 to 900 units, may correspond to additional electronic transitions or vibrational overtones. The presence of shoulder peaks and peak broadening, particularly noticeable in the bottom-left spectrum around 30-35 nm, indicates the potential presence of multiple absorbing species or a more complex molecular environment.

Overall, the spectra suggest that while all samples share a similar molecular framework, there are variations in concentration or environmental factors influencing the absorption characteristics. The top-left spectrum, with the highest overall absorbance, likely represents the sample with the highest concentration of the absorbing species, whereas the bottom-right spectrum reflects the lowest concentration. These UV-Vis spectra provide valuable insights into the molecular composition and concentration differences among the samples, highlighting the importance of UV-Vis analysis in characterizing the electronic transitions within various compounds.

.

# 3.4 Photoluminescence study

Photoluminescence emission spectra of pure and FZO films.

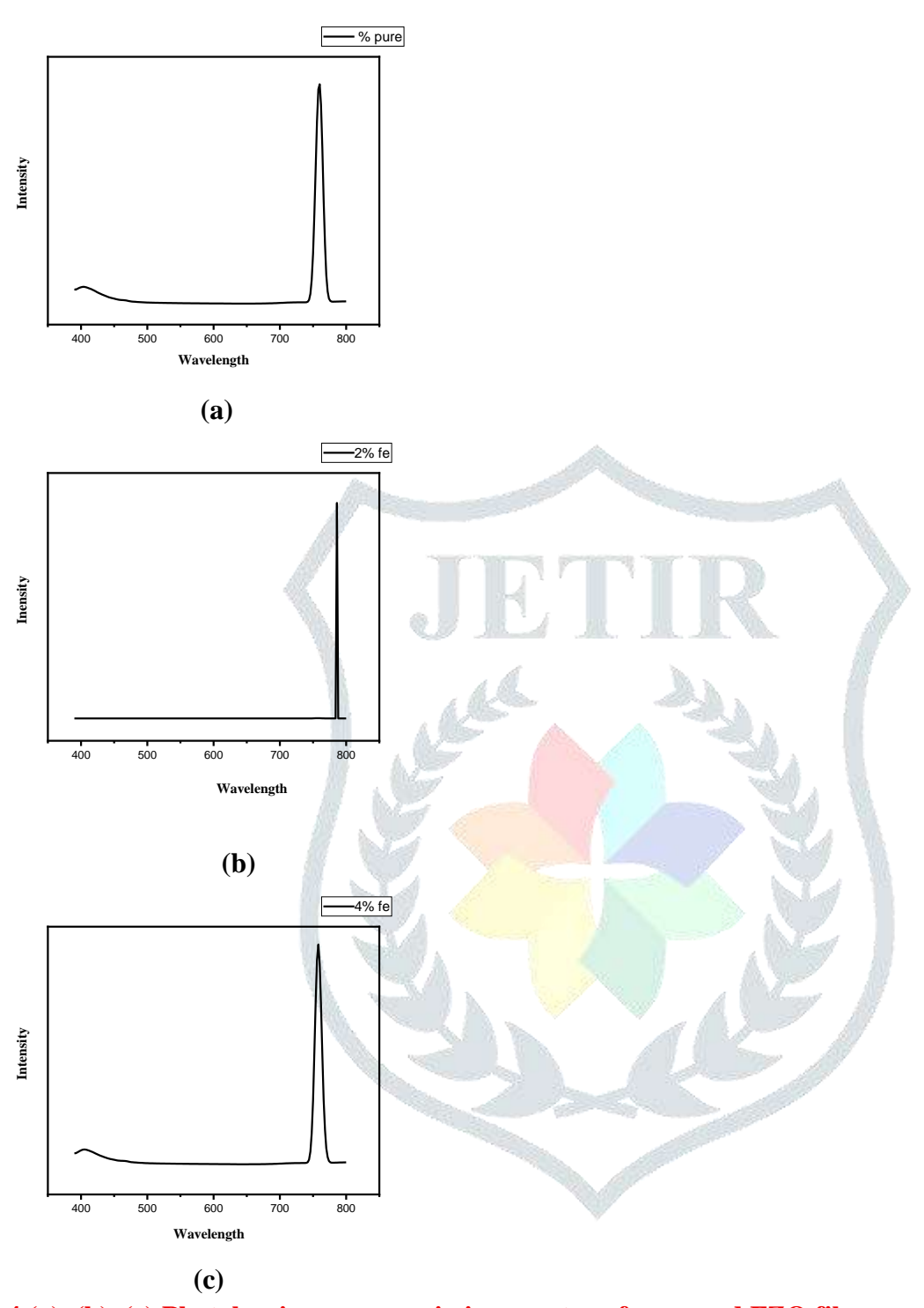


Fig.4 (a), (b), (c) Photoluminescence emission spectra of pure and FZO films.

In this study, the photoluminescence (PL) spectra were measured for all the FZO films at room temperature using a 330 nm light source. The PL results for pure ZnO and Fe-doped ZnO (FZO) films are shown in Fig. 8. For pure ZnO, a strong UV emission peak appeared at 382 nm. This UV emission happens because of the recombination of free excitons (electron-hole pairs).

When Fe was added to ZnO, the PL spectra showed changes. At first (for Fe up to 2 at.%), the UV peak shifted to a shorter wavelength, but for higher Fe levels (above 2 at.%), it shifted to a longer wavelength. At the same time, the intensity of the peak decreased as more Fe was added. These changes suggest that Fe doping affects the band gap of ZnO, and the decrease in peak intensity is due to the presence of Fe. Similar PL behavior in Fe-doped ZnO films has also been reported by Chen et al. using RF magnetron sputtering.[21]

### 4. Conclusion

In conclusion, zinc oxide (ZnO) is a semiconductor material that has garnered significant attention due to its unique properties, such as a wide band gap, high exciton binding energy, and excellent transparency and piezoelectricity. These characteristics make ZnO a highly versatile material for a wide range of applications, including optoelectronics, gas sensors, transparent conductive films, and photovoltaic devices. The potential of ZnO has been further expanded through the doping process, where various elements are introduced to modify and enhance its properties, particularly in the fields of magnetism, optics, and electronics.

Among the dopants, iron (Fe) has emerged as a particularly promising candidate due to its ability to introduce localized magnetic moments and significantly alter the electronic structure of ZnO. Fe doping in ZnO has shown potential for applications in spintronics and dilute magnetic semiconductors, where controlling the magnetic and electronic properties of materials is crucial. Additionally, Fe doping can also impact the optical band gap, defect states, and carrier concentration in ZnO, which could lead to improved performance in various devices, including sensors and photocatalysts.

The synthesis method used for Fe-doped ZnO thin films plays a critical role in determining their structural, morphological, and functional properties. Among the various methods, spray pyrolysis stands out as a versatile and cost-effective technique. It allows for the precise control of the film's composition, thickness, and uniformity, making it suitable for large-scale production. The spray pyrolysis process involves atomizing a precursor solution and directing it onto a heated substrate, where thermal decomposition occurs, resulting in the formation of thin films. The ability to optimize various parameters, such as substrate temperature, precursor concentration, and spray rate, allows for the tailoring of film characteristics to meet specific application requirements.

This study focused on the synthesis of nanostructured Fe-doped ZnO thin films using the spray pyrolysis method, followed by the characterization of their structural, morphological, and optical properties. The results demonstrated that Fe doping significantly influences the properties of ZnO thin films. X-ray diffraction (XRD) analysis confirmed that the Fe-doped ZnO films retained the hexagonal wurtzite structure of ZnO, with slight variations in peak intensities and positions indicating the incorporation of Fe into the ZnO lattice. The structural analysis also revealed that Fe doping affects the crystallite size, strain, and dislocation density of the films.

The optical properties, analyzed using UV-Visible spectroscopy, revealed that Fe doping led to a slight reduction in the optical band gap of ZnO, which could be attributed to the introduction of defect states and changes in the electronic structure caused by Fe incorporation.

The optical analysis exhibited higher optical absorbance with a slightly increased band gap for lower Fe-doped (1 at.%) films than the pure and highly doped films, which was supported by PL studies also.

Overall, the findings of this study contribute to the understanding of the relationship between synthesis conditions and the resulting properties of Fe-doped ZnO thin films. The successful synthesis and characterization of these films open up new possibilities for their application in advanced technological fields, particularly in optoelectronics, spintronics, and sensor devices. However, further research is needed to fully explore the longterm stability and performance of Fe-doped ZnO films in practical applications, as well as to optimize the doping levels and synthesis parameters to achieve the desired properties for specific uses.

### References

- [1] Vyas, S. (2020). A Short Review on Properties and Applications of Zinc Oxide Based Thin Films and Devices: ZnO as a promising material for applications in electronics, optoelectronics, biomedical and sensors. Johnson Matthey Technology Review, 64(2), 202–218. https://doi.org/10.1595/205651320x15694993568524
- [2] Muchuweni, E., Sathiaraj, T., & Nyakotyo, H. (2017). Synthesis and characterization of zinc oxide thin films for optoelectronic applications. Heliyon, 3(4), e00285. https://doi.org/10.1016/j.heliyon.2017.e00285
- [3] Ribut, S. H., Abdullah, C. a. C., & Yusoff, M. Z. M. (2019). Investigations of structural and optical properties of zinc oxide thin films growth on various substrates. Results in Physics, 13, 102146. https://doi.org/10.1016/j.rinp.2019.02.082
- [4] Han, C., Duan, L., Zhao, X., Hu, Z., Niu, Y., & Geng, W. (2019a). Effect of Fe doping on structural and optical properties of ZnO films and nanorods. Journal Alloys and Compounds, 770, 854-863. https://doi.org/10.1016/j.jallcom.2018.08.217

- [5] Lehru, R., Radhanpura, J., Kumar, R., Zala, D., Vadgama, V., Dadhich, H., Rathod, V., Trivedi, R., Pandya, D., Shah, N., & Solanki, P. (2021). Studies on electrical properties of Fe doped ZnO nanostructured oxides synthesized by sol-gel method. Solid State Communications, 336, 114415. https://doi.org/10.1016/j.ssc.2021.114415
- [6] Han, C., Duan, L., Zhao, X., Hu, Z., Niu, Y., & Geng, W. (2019b). Effect of Fe doping on structural and optical properties ZnO films and nanorods. Journal of Alloys and Compounds, 770. 854-863. https://doi.org/10.1016/j.jallcom.2018.08.217
- [7] Carofiglio, M., Barui, S., Cauda, V., & Laurenti, M. (2020). Doped Zinc Oxide Nanoparticles: Synthesis, Characterization and Potential Use in Nanomedicine. Applied Sciences, 10(15), 5194. https://doi.org/10.3390/app10155194 [8] Gudla, U. R., Suryanarayana, B., Raghavendra, V., Emmanuel, K., Murali, N., Taddesse, P., Parajuli, D., Naidu, K. C. B., Ramakrishna, Y., & Chandramouli, K. (2020). Optical and luminescence properties of pure, iron-doped, and glucose capped ZnO nanoparticles. Results in Physics, 19, 103508. https://doi.org/10.1016/j.rinp.2020.103508
- [9] Hareeshanaik, S., Prabhakara, M., Naik, H. B., Viswanath, R., Shivaraj, B., Vishnu, G., & Adarshgowda, N. (2023). Optical, photo catalytic, electrochemical and antibacterial performance of ZnO and Co doped ZnO nanoparticles. *Inorganic* Chemistry Communications, 158, 111552. https://doi.org/10.1016/j.inoche.2023.111552
- Gatou, M. A., Lagopati, N., Vagena, I. A., Gazouli, M., & Pavlatou, E. A. (2022). ZnO Nanoparticles from Different [10] Photocatalytic Potential Biomedical Use. Precursors and Their for Nanomaterials, *13*(1), 122. https://doi.org/10.3390/nano13010122
- Al-Rasheedi, A., Ansari, A. R., Abdeldaim, A. M., & Aida, M. S. (2022). Growth of zinc oxide thin films using [11] different precursor solutions by spray pyrolysis technique. The European Physical Journal Plus, 137(12). https://doi.org/10.1140/epjp/s13360-022-03599-2
- [12] Adachi, A., Ouadrhiri, F. E., Saleh, E. a. M., Althomali, R. H., Kassem, A. F., Ibtissam, E. M., Moharam, M. M., Husain, K., Eloutassi, N., & Lahkimi, A. (2023). Iron-doped catalyst synthesis in heterogeneous Fenton like process for dye degradation and removal: optimization using response surface methodology. SN Applied Sciences, 5(12). https://doi.org/10.1007/s42452-023-05543-0
- Pupilli, F., Tavoni, M., Drouet, C., Tampieri, A., & Sprio, S. (2024). Iron-doped Hydroxyapatite by hydrothermal [13] 100610. synthesis: factors modulating the Fe2+, Fe3+ content. Open Ceramics, 18, https://doi.org/10.1016/j.oceram.2024.100610
- Srinivasulu, T., Saritha, K., & Reddy, K. R. (2017b). Synthesis and characterization of Fe-doped ZnO thin films [14] deposited pyrolysis. Electronic Materials, 76-85. chemical spray Modern 3(2),https://doi.org/10.1016/j.moem.2017.07.001
- Zhang, X., Wang, J., Ma, J., & Hu, J. (2016). Preparation and characterization of ZnO and Fe-doped ZnO films by sol-gel method. DOAJ (DOAJ: Directory of Open Access Journals). https://doi.org/10.7535/hbkd.2016yx02011
- Ranathunga, K., Yapa, P., Munaweera, I., Weerasekera, M. M., & Sandaruwan, C. (2024). Preparation and [16] characterization of Fe-ZnO cellulose-based nanofiber mats with self-sterilizing photocatalytic activity to enhance antibacterial applications under visible light. RSC Advances, 14(26), 18536–18552. https://doi.org/10.1039/d4ra03136a
- Umar, S., & Kumar, M. (2018). Effect of Fe doping on optical and structural properties of ZnO thin film prepared [17] by spray pyrolysis method. Materials Today Proceedings, 5(3), 9173-9176. https://doi.org/10.1016/j.matpr.2017.10.039
- [18] Reza, G. H., Mahboobeh, S., Ali, S. M., & Morad, R. A. (2011). Synthesis of ZnO Nanoparticles by Spray Pyrolysis Method. Iranian Journal of Chemistry & Chemical Engineering-international English Edition, 30(157), 1-6. https://doi.org/10.30492/ijcce.2011.6250
- Srinivasulu, T., Saritha, K., & Reddy, K. (2017a). STRUCTURAL AND PHOTOLUMINESCENCE [19] PROPERTIES OF Fe-DOPED ZnO THIN FILMS. International Journal of Advanced Research, 5(4), 958-963. https://doi.org/10.21474/ijar01/3902
- [20] A. Parra-Palomino, O. Perales-Perez, R. Singhal, M. Tomar, Jinwoo Hwang, P.M. Voyles, Structural, optical and magnetic characterization of monodisperse Fe doped ZnO nanocrystals, J. Appl. Phys. 103 (2008) [07D121-1 to 3].
- [21] A. Gotkas, I.H. Mutlu, Y. Yamada, Influence of Fe-doping on the structural, optical and magnetic properties of ZnO thin films prepared by sol-gel method, Superlattices Microstruct. 57 (2013) 139–149.
- [22] A.J. Chen, X.M. Wu, Z.D. Sha, L.J. Zhuge, Y.D. Meng, Structure and photolumi nescence properties of Fedoped ZnO thin films, J. Phys. D: Appl. Phys. 39 (2006) 4762–4765.